DIABETES/METABOLISM RESEARCH AND REVIEWS
Diabetes Metab Res Rev 2005; **21**: 367–375.
Published online 3 December 2004 in Wiley InterScience (www.interscience.wiley.com). **DOI:** 10.1002/dmrr.527

RESEARCH ARTICLE

Endothelin-mediated remodeling in aortas of diabetic rats

Gen Fukuda[1]
Zia A. Khan[1]
Yousef P. Barbin[1]
Hana Farhangkhoee[1]
Ronald G. Tilton[2]
Subrata Chakrabarti[1]*

[1]*Department of Pathology, University of Western Ontario, London, ON, Canada*

[2]*Department of Internal Medicine, University of Texas Medical Branch, Galveston, Texas, USA*

*Correspondence to: Subrata Chakrabarti, Department of Pathology, Dental Sciences Building, University of Western Ontario, London, Ontario. N6A 5C1, Canada.
E-mail: schakrab@fmd.uwo.ca

Received: 7 May 2004
Revised: 20 August 2004
Accepted: 5 September 2004

Abstract

Background Smooth muscle cells proliferation and extracellular matrix (ECM) protein deposition are key features of diabetic macroangiopathy. In the present study, we have studied the role of endothelin$_A$ (ET_A) receptor, the predominant receptor on smooth muscle cells, in diabetes-induced vascular hypertrophy and remodeling.

Methods Streptozotocin-induced diabetic rats were administrated a selective ET_A receptor antagonist, TBC3214, for 26 weeks. Following treatment, aortas were harvested and subjected to gene expression and morphometric analyses. We quantified fibronectin (FN) and plasminogen activator inhibitor-1 (PAI-1) expression as indicators of increased ECM protein synthesis. ET-1, ET-3, transforming growth factor-β1 (TGF-β1) and angiotensinogen mRNA levels were measured to elucidate genes involved in FN expression. We have investigated an embryonic splice variant of FN, oncofetal FN, and nonmuscle myosin heavy chain (SMemb) as vascular remodeling indicators.

Results Our results show that diabetes leads to upregulation of FN, PAI-1, ET-1, ET-3, TGF-β1 and angiotensinogen mRNA levels in association with increased medial thickness. Immunohistochemical analyses revealed concurrent protein level changes. Diabetes also upregulated oncofetal FN and SMemb mRNA levels. Treatment with TBC3214 attenuated the mRNA levels of several genes and prevented increased medial thickness.

Conclusions These results indicate that diabetes-induced vascular hypertrophy and remodeling is associated with reexpression of embryonic forms of FN and myosin heavy chain. Such changes are ET-dependent and may be mediated via TGF-β1 and angiotensin.

Keywords macroangiopathy; endothelins; extracellular matrix; oncofetal fibronectin; SMemb

Introduction

Large vessel disease or macroangiopathy is the leading cause of mortality in diabetic patients [1,2]. Augmented atherosclerotic process, pathologically manifested as arterial narrowing due to medial calcification

and thickening, is the cardinal feature of diabetic macroangiopathy [3]. Increased deposition of extracellular matrix (ECM) protein and proliferation of vascular smooth muscle cells are key structural and functional components of diabetes-induced vascular hypertrophy and remodeling. We and others have previously demonstrated that glucose-induced increased ECM protein synthesis, such as collagen 1α (IV) and fibronectin (FN), in endothelial cells as well as in target organs of diabetic complications is mediated, at least in part, via an endothelin (ET) dependent mechanism [4–10].

Fibronectin is a predominant protein in the ECM [11,12]. FN plays important roles in various cellular events including cell adhesion, motility, and tissue repair. Several factors may influence augmented FN synthesis in diabetes. Among these factors, fibrogenic proteins like ETs, transforming growth factor-β (TGF-β1), and angiotensin II (Ang II) have gained significant attention because of their ability to strongly upregulate ECM protein synthesis [8,13–16]. Mechanisms of ECM accumulation may, however, involve increased synthesis of FN and collagen along with decreased degradation through upregulation of inhibitors of ECM proteases such as plasminogen activator inhibitor-1 (PAI-1) [13]. In addition to increased synthesis, FN has been shown to undergo alternative splicing to produce embryonic isoforms in various pathological conditions such as fibrotic diseases and tumorogenesis [17,18]. One such splice variant, EDB^+ oncofetal FN, has been shown to be exclusively expressed in proliferating tissues during embryogenesis. Upregulation of oncofetal FN, which is absent in normal adult tissues, is potentially an important phenomenon in tissue repair and tumor angiogenesis [19,20]. We have previously demonstrated upregulation of oncofetal FN in the retinas of diabetic rats via an ET-dependent pathway [21].

In addition to upregulated ECM proteins, vascular hypertrophy also entails cellular hypertrophy and hyperplasia. Smooth muscle cells are indispensable in these pathogenic changes as these are the only cell types that inhabit the medial layer of the vascular tissue. A key morphological change observed in various models of vascular injury is phenotypic switch of vascular smooth muscle cells from contractile to synthetic type. This switch of smooth muscle cells to a fibroblast-like phenotype has been associated with reexpression of embryonic form of myosin heavy chain (SMemb) [22,23]. Aberrant expression of SMemb has been demonstrated in both experimental and human atherosclerotic lesions [24,25].

In the present study, we have investigated whether diabetes-induced vascular hypertrophy in the rat aorta is associated with an imbalance between ECM protein synthesis and degradation, and whether such changes are associated with a dedifferentiated state leading to oncofetal FN and SMemb reexpression. Furthermore, we examined the role of ET system and its possible interaction with TGF-β1 and Ang II in diabetes-induced vascular remodeling.

Methods

Induction of diabetes and administration of TBC3214

Male Sprague-Dawley rats weighing approximately 270 to 290 g were made diabetic by a single intravenous injection of streptozotocin (60 mg/kg in 0.3 mL citrate buffer) [7,8]. Animals were monitored with respect to plasma glucose and glycated hemoglobin levels, body weight, urine volume, water and food consumption, and glucose and ketone levels. Diabetic rats with nonfasting plasma glucose values exceeding 22.2 mmol/L and/or with a weight loss exceeding 10% of initial body weight were placed on low-dose insulin therapy. Ten units/kg body weight of NPH human insulin were administered subcutaneously, and discontinued if body weights recovered and nonfasting plasma glucose values remained below 22.2 mmol/L. Age- and sex-matched rats were used as controls (CO, $n = 8$) and were given equal volume of citrate buffer. Diabetic rats were randomly divided into two groups, diabetic rats (DM, $n = 7$) and diabetic rats on selective endothelin$_A$ (ET_A) receptor antagonist, TBC3214 (DM-TBC, $n = 13$) (30 mg/kg/day mixed with water) [26]. TBC3214 is a highly selective ET_A receptor antagonist developed from sitaxsetan (TBC11251) with an acyl group modification at the 2-position of the anilide to improve the bioavailability [27].

Rats were treated for 26 weeks. We have previously reported cardiovascular structural changes 6 months following onset of diabetes [6]. Rats were euthanized and the pleural cavity aortas were obtained. Blood pressures were measured by cannulating abdominal aorta distal to renal arteries. Portions of tissues were frozen for RNA extraction and remaining were fixed in 10% formalin and embedded in paraffin for morphometric analysis.

All rats were treated and cared for in accordance with the National Institutes of Health Guide for the Care and Use of Laboratory Animals (National Research Council, Washington, 1996) and in compliance with the United States Department of Agriculture regulations, and the American Veterinary Medicine Association's Panel on Euthanasia guidelines.

Measurement of medial thickness

Five micrometer sections of paraffin embedded tissues were transferred to glass slides and subjected to elastic trichrome-stain using routine histochemical methods. Orthogonal intercept method was used for detecting medial thickness [28,29]. At each point of intersection of the overlying grid, the distance between innermost and outermost elastic lamia was measured and the value for each vessel was obtained using a computer-assisted image analysis system (Mocha Image Analysis Software; Jandel Scientific, CA, USA).

Immunohistochemical analysis

Five micrometers sections on positively charged slides were used for immunohistochemical analysis using antibodies ET-1, ET-3 (1 : 500, polyclonal, Pennsylvania Laboratories), TGF-β1 (1 : 500, polyclonal, Promega Corporation) and FN (1 : 500, polyclonal, DAKO Diagnostics Canada). A streptavidin–biotin peroxidase technique was used as previously described [5,6,7]. Negative controls included replacement of primary antibody with nonimmune serum. The slides were counterstained by hematoxylin and were analyzed in a masked fashion.

RNA isolation and cDNA synthesis

Total RNA was isolated from frozen tissue sections using TRIzol™ (Invitrogen Inc. Burlington, Ontario, Canada) reagent [4,8,28]. Following addition of chloroform, samples were centrifuged to separate aqueous and organic phases. RNA was recovered from the aqueous phase by isopropyl alcohol precipitation and suspended in DEPC-treated water. RNA was quantified by measuring UV absorbance at 260 nm. Purity of samples was determined by calculating ratio of absorbance at 260 nm and 280 nm.

Four micrograms of total RNA was used for cDNA synthesis using the Superscript-II™ system (Invitrogen Inc.). Briefly, RNA was added to Oligo (dT) primers and denatured at 70 °C for 10 min. Reverse transcription was carried out by addition of MMLV reverse transcriptase and incubation of samples at 42 °C for 55 min. The resulting cDNA products were stored at −20 °C.

Real-time RT-PCR

Real-time RT-PCR was carried out in the LightCycler™ (Roche Diagnostics Canada, PQ, Canada) using SYBR Green I [30]. PCR reactions were performed in microcapillary tubes (Roche Diagnostics Canada) with a final volume of 20 µL. The reaction mixture consisted of 2.5 µL of 10X PCR buffer (Invitrogen Inc.), 1.25 µL of 5 mmol/L dNTP, 1.2 µL of 50 mmol/L $MgCl_2$ (1.6 µL for ET-1), 1 µL of each forward and reverse 10 µmol/L primers, 0.5 µL of 5 units/µL Platinum Taq polymerase, 0.75 µL of 10X SYBR Green I (Molecular Probes, Eugene, OR, USA), 10.8 µL H_2O and 1 µL cDNA template.

Primers for all genes were designed in accordance with LightCycler guidelines (Table 1; Ref. 31). Primers for total FN were designed to include all possible splice variants of FN. In addition, because of the small product size of Ang II, primers were designed to amplify and quantitate angiotensinogen, precursor of Ang II, for the assessment of Ang II expression. During PCR reactions, an additional step (signal acquisition phase) was incorporated following

Table 1. Primer sequences and temperature profiles for real-time RT-PCR

Primer sequences (5′ → 3′)	PCR parameters temperature – time (temperature ramp rate[a])	
Total FN	Annealing	60 °C – 5 s
CCAGGCACTGACTACAAGAT	Extension	72 °C – 17 s
CATGATACCAGCAAGGACTT	Signal	84 °C – 1 s
Oncofetal FN	Annealing	55 °C – 5 s
CCGCCATTAATGAGAGTGAT	Extension	72 °C – 8 s
AGTTAGTTGCGGCAGGAGAAG	Signal	81 °C – 1 s
Smemb	Annealing	55 °C – 5 s
CAGGAGTTCAGACAGAGATA	Extension	72 °C – 10 s
CTCTTTCTTCCTCTAAGTGC	Signal	82 °C – 1 s
ET-1	Annealing	58 °C – 5 s
GCTCCTGCTCCTCCTTGATG	Extension	72 °C – 20 s
CTCGCTCTATGTAAGTCATGG	Signal	84 °C – 1 s
ET-3	Annealing	45 °C – 5 s
GCACTTGCTTCACTTATAAGG	Extension	72 °C – 17 s (4 °C/s)
ACAGAAGCAAGAAGCATCAGTTG	Signal	84 °C - 1 s
TGF-β1[31]	Annealing	59 °C – 5 s
GTAGCTCTTGCCATCGGG	Extension	72 °C – 12 s
GAACGTCCCGTCAACTCG	Signal	85 °C – 1 s
Angiotensinogen	Annealing	50 °C - 5 s
ATCTTCTGCATCCTGACCT	Extension	72 °C – 10 s (5 °C/s)
GCACAGGCTCAAAGGTT	Signal	85 °C – 1 s
PAI-1	Annealing	58 °C – 5 s
TCCACAAGTCTGATGGTAGC	Extension	72 °C – 9 s
GTTGCTCTTCCATTGTCTGA	Signal	84 °C – 1 s
β actin	Annealing	58 °C – 5 s
CCTCTATGCCAACACAGTGC	Extension	72 °C – 8 s
CATCGTACTCCTGCTTGCTG	Signal	83 °C – 1 s

Initial denaturation period was 1 min at 95 °C.
[a]Ramp rate was 20 °C/s unless otherwise mentioned.

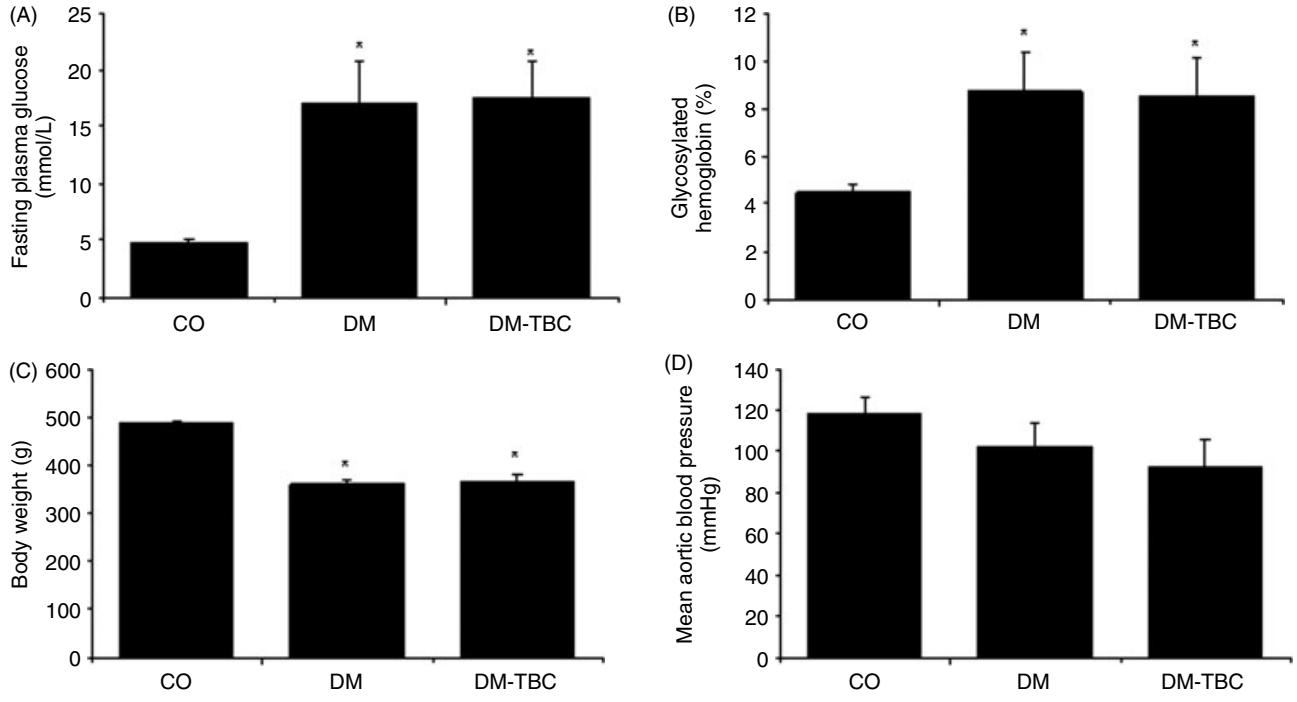

Figure 1. Clinical monitoring of animals. Biophysical parameters of animals showing, (A) fasting plasma glucose, (B) glycated hemoglobin levels, (C) body weight gain, and (D) mean aortic blood pressure. Poorly controlled diabetic rats (DM) demonstrated hyperglycemia, increased glycated hemoglobin levels and reduced body weight gain compared to controls (CO). TBC3214 treatment (DM-TBC) had no effect on these parameters. Mean aortic blood pressure showed no alterations in any of the groups (* = significantly ($p < 0.05$) different as compared to CO)

the extension phase to minimize interference from nonspecific signals [32]. Temperature profiles used for RT-PCR are given in Table 1. mRNA levels were quantified using standard curve method. Standard curves were constructed using serially diluted standard template. Cp value (crossing point; log-linear phase) was used to compute mRNA levels from the standard curves. mRNA levels were normalized to β-actin to account for differences in reverse transcription efficiencies and amount of cDNA in reaction mixtures. Oncofetal FN was normalized to total FN to determine relative change in expression of oncofetal FN.

Statistical analysis

The data are expressed as mean ± SEM and were analyzed by ANOVA followed by Tukey's post-hoc test. Differences were considered significant at values of $p < 0.05$.

Results

Clinical monitoring of animals

Diabetes was confirmed by blood glucose estimation. Poorly controlled diabetic animals demonstrated hyperglycemia and increased glycated hemoglobin levels, and reduced body weight gain (Figure 1). Both diabetic groups showed increased urinary output (CO 16 ± 8 mL/day, DM $^*196 \pm 48$ mL/day, DM-TBC $^*204 \pm 39$ mL/day, $^*p < 0.05$), increased food (CO 23 ± 3 mg/day, DM $^*44 \pm 9$ mg/day, DM-TBC $^*52 \pm 6$ mg/day, $^*p < 0.05$) and water consumption (CO 44 ± 14 mL/day, DM $^*269 \pm 33$ mL/day, DM-TBC $^*256 \pm 49$ mL/day, $^*p < 0.05$) compared to control rats. These data are indicative of diabetic dysmetabolism in these animals. TBC3214 treatment of the diabetic rats had no effects on these parameters. We monitored the animals daily and treated them with low-dose insulin as necessary to prevent excessive body weight loss and ketosis. Although the possibility of mild ketosis affecting the observed changes cannot be excluded, we believe that such changes are minimal. Mean aortic blood pressure, measured by cannulating abdominal aorta, showed no significant alterations in any of the groups, although it tended to be slightly lower in diabetic animals (Figure 1).

Diabetes-induced increased expression of FN and PAI-1 in aortas

One of the key structural components of increased vascular medial thickness is ECM protein deposition. ECM accumulation results from upregulated expression and decreased degradation of proteins [13]. Therefore, we have quantified mRNA levels of FN, a key ECM protein, and PAI-1, a predominant inhibitor of ECM protein degradation. It should be noted, however, that an implicit assumption is that the level of an mRNA is a reliable indicator of the level of its protein product. We have previously demonstrated that mRNA alteration parallels

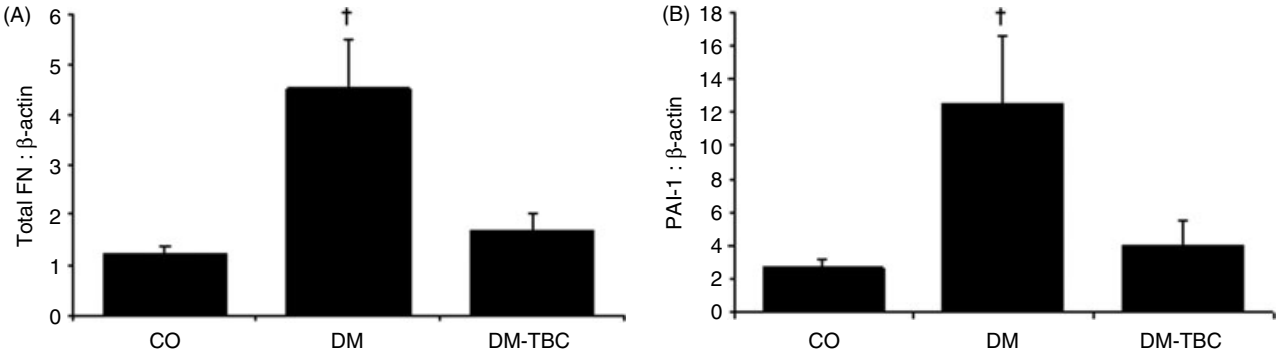

Figure 2. mRNA expression of total FN and PAI-1. Quantitative mRNA expression of (A) total FN, and (B) PAI-1, using real-time RT-PCR showing significant increase of these transcripts in the aorta of diabetic (DM) rats compared to controls (CO) and diabetic rats on TBC3214 (DM-TBC). († = significantly different as compared to CO and DM-TBC; $p < 0.05$)

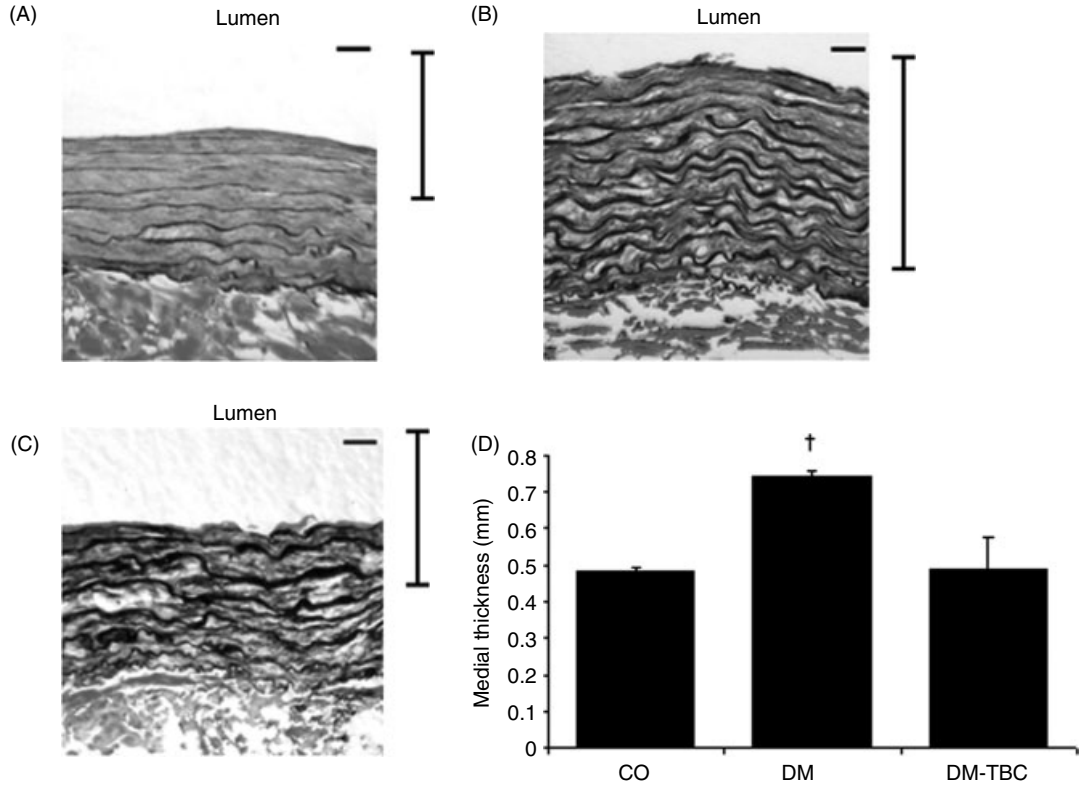

Figure 3. Medial thickness of rat aortas. Representative elastic trichrome stained aortic sections from (A) control rats, (B) diabetic rats, and (C) diabetic rats on TBC3214 (Vertical bar represents area measured for quantitative analysis). (D) quantitative measurement of medial thickness of diabetic (DM) rats compared to controls (CO) and diabetic rats on TBC3214 (DM-TBC). (Scale bar represents 0.1 mm, † = significantly different as compared to CO and DM-TBC; $p < 0.05$)

protein expression [21]. Our results indicate increased expression of FN in aortas of diabetic rats as compared to controls (Figure 2A). Treatment with ET_A receptor antagonist normalized the levels of total FN in diabetic rats. In addition, PAI-1 mRNA levels were found to be increased in aortas of diabetic rats (Figure 2B). TBC3214 reduced the levels of PAI-1 indicating an important role of ET signaling in increased ECM production and decreased degradation in diabetes-induced vascular hypertrophy.

Prevention of medial thickening by ET_A antagonism

Increased production and decreased degradation of ECM proteins should lead to thickening of the vessel walls. Hence, we performed morphometric analysis, which demonstrated significant thickening of medial layer of the diabetic rat aortas as compared to control (Figure 3A and B). Treatment with ET_A receptor selective antagonist, TBC3214, significantly reduced medial wall thickness to

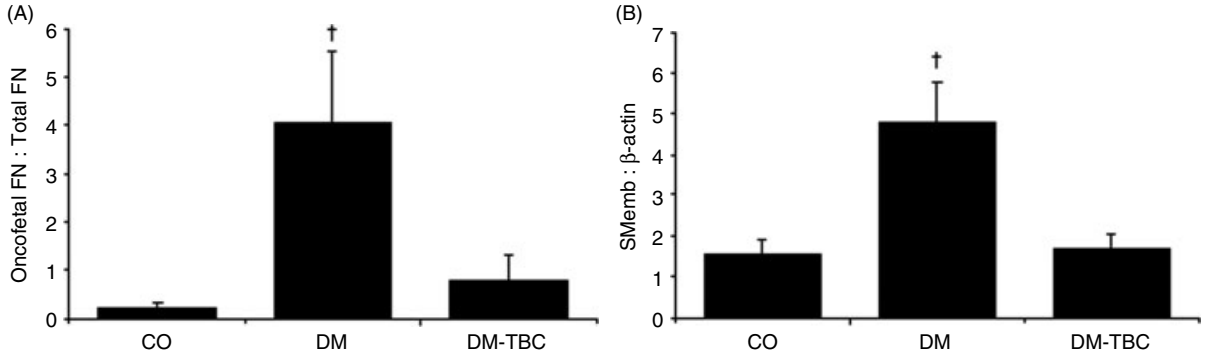

Figure 4. mRNA expression of oncofetal FN and Smemb. Quantitative mRNA expression of, (A) oncofetal FN, and (B) SMemb showing significant increase of transcripts in the aorta from diabetic (DM) rats compared to controls (CO) and diabetic rats on TBC3214 (DM-TBC). Oncofetal FN mRNA levels are expressed as ratio of target mRNA to total FN. [† = significantly different as compared to CO and DM-TBC; $p < 0.05$]

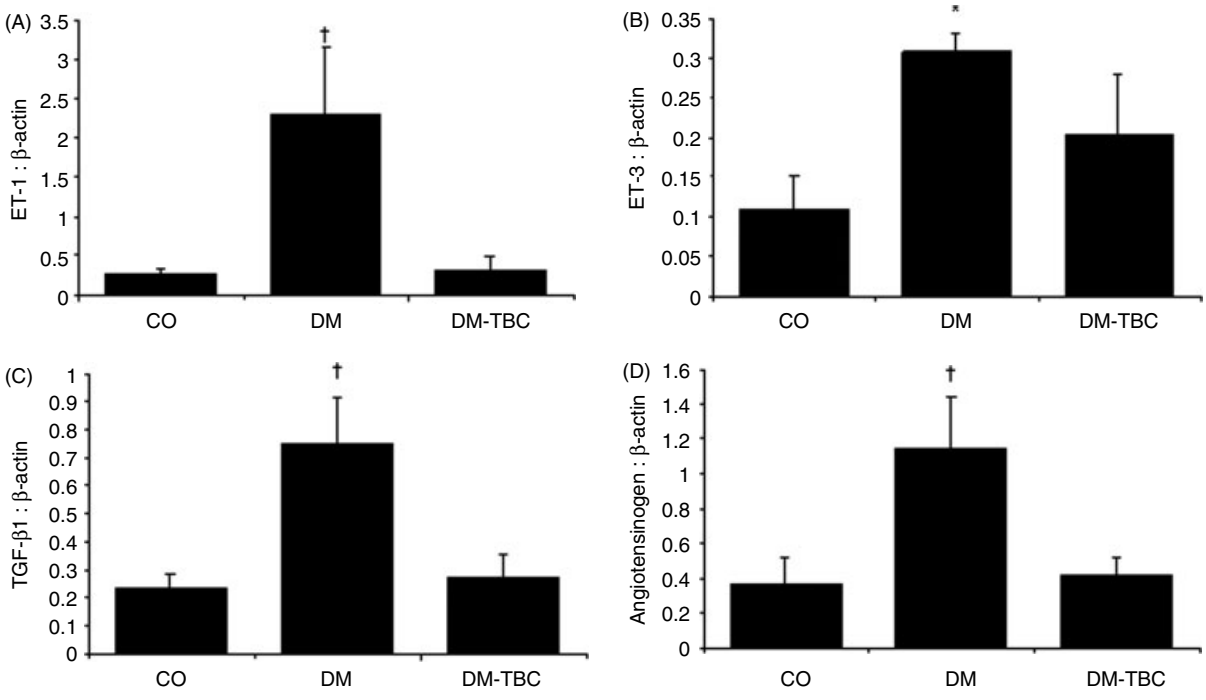

Figure 5. mRNA expression of ET-1, ET-3, TGF-β1 and angiotensinogen. Quantitative mRNA expression of (A) ET-1, (B) ET-3, (C) TGF-β1 and (D) angiotensinogen using real-time RT-PCR, showing significant increase of all transcripts in the aorta from diabetic (DM) rats compared to controls (CO). († = significantly different as compared to CO and DM-TBC, * = significantly different as compared to CO; $p < 0.05$)

levels approaching those in control rats (Figure 3). These data are indicative of a potential role of ET_A receptor signaling in diabetes-induced vascular hypertrophy.

ET_A signaling in aberrant reexpression of embryonic forms of FN and myosin heavy chain

Expression of embryonic isoforms of various proteins may be important in remodeling. In the context of vascular tissue remodeling, the important proteins exhibiting embryonic form are cytoskeletal and ECM proteins [21–23,33]. We have evaluated oncofetal FN, an embryonic splice variant of FN believed to be involved in tissue repair, and SMemb, a key cytoskeletal protein representative of smooth muscle phenotypic change [22,23]. Our data indicates that both of these fetal forms are upregulated in aortas of diabetic rats (Figure 4A and B). TBC 3214 significantly decreased the levels of these embryonic forms to levels similar to control. Our data strongly suggests that ET receptor mediated signaling may be involved in reexpression of embryonic forms of these proteins, which could regulate the proliferative and migratory behavior of cells.

Diabetes-induced upregulation of ETs, TGF-β1 and angiotensinogen

We have previously demonstrated that hyperhexosemia-induced ET expression is an important mediator of

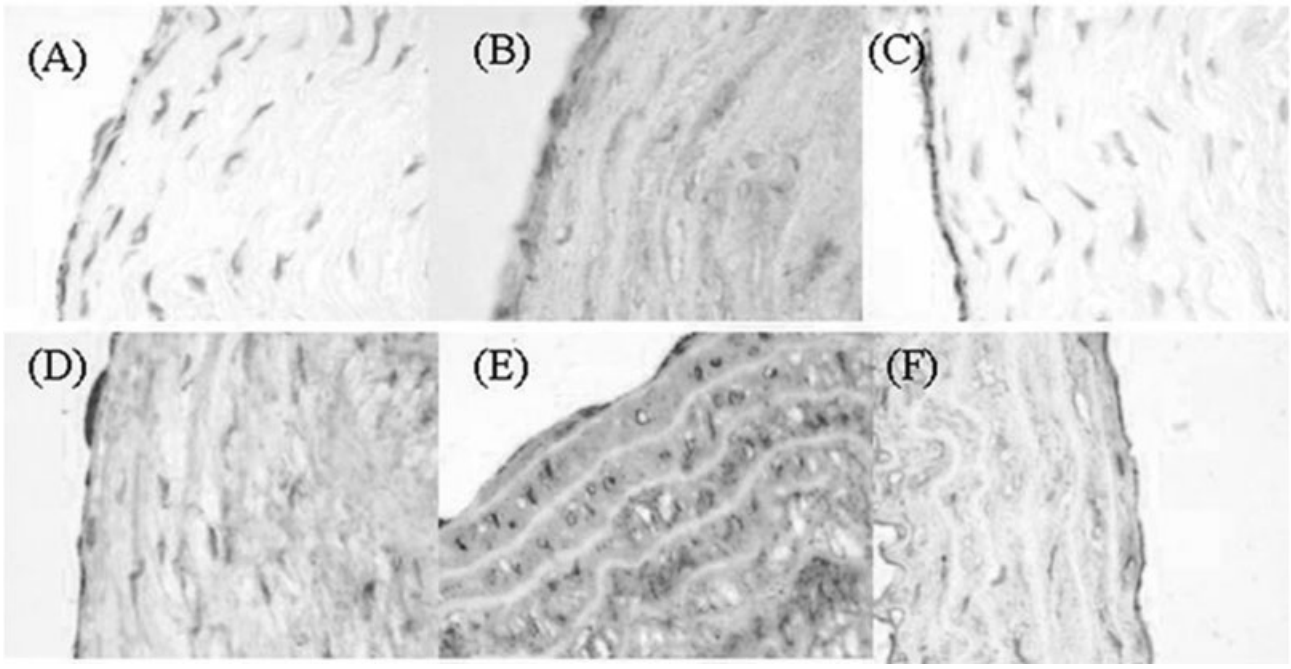

Figure 6. Immunohistochemical analysis of ET-1 and FN. Immunohistochemical analysis of ET-1 (A–C) and FN (D–F) in the rat aorta from (A) and (D) control animals (CO), (B) and (E) diabetic animals (DM) and (C) and (F) diabetic animals on TBC3214 (DM-TBC). An increase in immunostaining was observed in DM and was decreased to normal levels in DM-TBC. Please note that a similar pattern was observed with ET-3 and TGF-β1 staining (data not shown). (Original magnification ×400, slides were counterstained with hematoxylin)

increased ECM protein production in diabetes [7,8]. In order to elucidate the signaling pathways involved in ECM accumulation and oncofetal FN and SMemb expression, we have studied the expression of potential mediators involved in vascular hypertrophy and remodeling. Diabetes caused a significant increase in ET-1 mRNA expression in aortas of rats (Figure 5A). ET-3 also exhibited a similar increase in diabetes (Figure 5B). TBC3214 treatment reduced ET-1 expression but not ET-3 expression in aortas of diabetic rats in accordance with previous findings [34], suggesting that ET_A receptors have higher affinity for ET-1 compared to ET-3. TGF-β1 and angiotensinogen mRNA levels showed a similar increase as ET-1 in diabetic rats (Figure 5C and D). Treatment with TBC3214 reduced mRNA levels of both TGF-β1 and angiotensinogen, indicating a significant role of ET signaling in upregulation of these fibrogenic genes.

In parallel to the increasing mRNA expression levels, immunohistochemical analysis demonstrated increased staining of the peptides in the aorta, which were reduced by TBC3214 treatment (Figure 6).

Discussion

In the present study, we have, for the first time, demonstrated that diabetes-induced medial thickening of the aorta is associated with reexpression of two embryonic genes, namely, oncofetal FN and SMemb along with increased total FN mRNA expression. We have further demonstrated that ETs may arbitrate such alterations via regulation of potent fibrogenic factors such as TGF-β1, angiotensinogen and PAI-1. We have carried out these studies in streptozotocin-induced diabetic rat, which is a well-studied model of diabetic complications [5–7]. The characteristic vascular hypertrophic changes in diabetes have previously been demonstrated in this model [35].

This study demonstrated upregulation of EDB^+ oncofetal FN, alongside total FN, in aortas of diabetic rats. Oncofetal FN is normally absent in mature adult tissues. However, oncofetal FN has been shown to be reexpressed in tissues during remodeling as well as during tumor angiogenesis [17–20]. This isoform has also been associated with higher proliferative index of vascular endothelial cells [36]. The role of this aberrant FN isoform in the pathogenic changes of diabetic complications is obscure. However, evidence from nondiabetic situations suggests that oncofetal FN may be important in increasing cellular proliferation and migration [36,37]. Indeed, oncofetal FN has been shown to promote cell adhesion,which could facilitate cell proliferation and migration [37]. We have previously demonstrated that oncofetal FN may regulate vascular endothelial cell proliferation [21]. In accordance with the findings of the present study, previous data from our laboratory show that diabetes-induced oncofetal FN production in the retina is regulated by ETs [21]. The current findings in large vessel would suggest that oncofetal FN and SMemb production may play a part in diabetic vasculopathy. It is of interest to note that both diabetic animals tended to show a nonsignificant lowering of blood pressure compared to control animals. Hence,

in the present study the effect of ET antagonism were possibly not medicated via reduction of blood pressure.

The role of ETs in vascular hypertrophy was initially suggested by experimental evidence of increased synthesis and release of ETs from mesenteric vessels of diabetic rats [38]. We and others have demonstrated increased ET production in several target organs of diabetic complications [5,6,8,39]. Recent studies have further confirmed increased ET expression in intimal and adventitial layers of mesenteric arteries [40]. This increase has been associated with ECM protein accumulation and upregulation of other fibrogenic proteins like TGF-β1 [41]. In addition, *in vitro* studies indicate that Ang II-induced vascular hypertrophy can be attenuated by ET receptor antagonism [40]. It has also been demonstrated that Ang II can promote prepro-ET expression as well as processing [42]. Treatment of diabetic rats with ACE inhibitors or Ang II receptor antagonists attenuate diabetes-induced mesenteric vascular hypertrophy [43,44]. These findings suggest an intricate interrelationship between these fibrogenic proteins in mediating diabetes-induced vascular remodeling. Our data confirms such an interaction by which blockade of ET_A receptor mediated signaling lead to normalization of TGF-β1 and angiotensinogen.

ETs and Ang II have also been shown to be involved in vascular remodeling through their mitogenic actions on smooth muscle cell [45–49]. The role of ET signaling in vascular smooth muscle cell proliferation has been confirmed in studies that show ability of ET_A receptor antagonists to prevent smooth muscle cell proliferation in restenosis and atherosclerosis, mesangial cell proliferation in glomerulonephritis, and fibrosis in cardiac failure [44–49]. This higher proliferative index of smooth muscle cells is represented by phenotypic switch from contractile to synthetic type. An important molecular marker of such a change is increased reexpression of SMemb. SMemb has been shown to be upregulated in myocardium in diabetes [50] and also by hyperglycemia in rat mesangial cells [51]. In keeping with such findings, we have demonstrated that upregulation of SMemb expression in aortas of diabetic rats is dependent on ET receptor mediated signaling.

In summary, we have demonstrated that diabetes-induced aortic medial hypertrophy is associated with a state of relative dedifferentiation as evidenced by increased mRNA expression of oncofetal FN and SMemb. We have further demonstrated that these changes are mediated by ET, which may stimulate a remodeling phenomenon by increasing fibrogenic molecules, TGF-β1 and angiotensinogen and production of total FN. Further studies are necessary to examine whether increased oncofetal FN may provide a potential molecular target for adjuvant therapy.

Acknowledgements

This study was supported by research grants from Canadian Diabetes Association in honor of the late Glenn W. Liebrock, Canadian Institutes of Health Research, and Lawson Health Research Institute.

References

1. Gray RP, Yudkin JS Cardiovascular disease in diabetes mellitus. In *Textbook of Diabetes* (2nd edn), Pickup JC, Williams G (eds). Oxford: Blackwell Science, 1997; 57.1–57.22.
2. Stamler J, Vaccaro O, Neaton JD, Wentworth D. Diabetes, other risk factors, and 12-yr cardiovascular mortality for men screened in the multiple risk factor intervention trial. *Diabetes Care* 1993; **16**: 434–444.
3. Neubauer B, Christensen NJ, Christensen T, Gundersen HJ, Jorgensen J. Diabetic macroangiopathy. Medial calcifications, narrowing, rugosities, stiffness, norepinephrine depletion and reduced blood flow capacity in the leg arteries. *Acta Med Scand Suppl* 1984; **687**: 37–45.
4. Chen S, Mukherjee S, Chakraborty C, Chakrabarti S. High glucose-induced, endothelin-dependent fibronectin synthesis is mediated via NF-κB and AP-1. *Am J Physiol Cell Physiol* 2003; **284**: 263–272.
5. Chen S, Evans T, Deng D, Cukiernik M, Chakrabarti S. Hyperhexosemia induced functional and structural changes in the kidneys: role of endothelins. *Nephron* 2002; **90**: 86–94.
6. Chen S, Evans T, Mukherjee K, Karmazyn M, Chakrabarti S. Diabetes-induced myocardial structural changes: role of endothelin-1 and its receptors. *J Mol Cell Cardiol* 2000; **32**: 1621–1629.
7. Deng D, Evans T, Mukherjee K, Downey D, Chakrabarti S. Diabetes-induced vascular dysfunction in the retina: role of endothelins. *Diabetologia* 1999; **42**: 1228–1234.
8. Evans T, Deng DX, Chen S, Chakrabarti S. Endothelin receptor blockade prevents augmented extracellular matrix component mRNA expression and capillary basement membrane thickening in the retina of diabetic and galactose-fed rats. *Diabetes* 2000; **49**: 662–666.
9. Roy S, Cagliero E, Lorenzi M. Fibronectin overexpression in retinal microvessels of patients with diabetes. *Invest Ophthalmol Vis Sci* 1996; **37**: 258–266.
10. Nakamura T, Ebihara I, Fukui M, Tomino Y, Koide H. Effect of a specific endothelin receptor A antagonist on mRNA levels for extracellular matrix components and growth factors in diabetic glomeruli. *Diabetes* 1995; **44**: 895–899.
11. Yamada KM. Cell surface interactions with extracellular materials. *Annu Rev Biochem* 1983; **52**: 761–799.
12. Kornblihtt AR, Umezawa K, Vibe-Pedersen K, Baralle FE. Primary structure of human fibronectin: differential splicing may generate at least 10 polypeptides from a single gene. *EMBO J* 1985; **4**: 1755–1759.
13. Border WA, Noble N. Transforming growth factor-beta in tissue fibrosis. *N Engl J Med* 1994; **331**: 1286–1292.
14. Fornoni A, Striker LJ, Zheng F, Striker GE. Reversibility of glucose-induced changes in mesangial cell extracellular matrix depends on the genetic background. *Diabetes* 2002; **51**: 499–505.
15. Fakhouri F, Placier S, Ardaillou R, Dussaule JC, Chatziantoniou C. Angiotensin II activates collagen type I gene in the renal cortex and aorta of transgenic mice through interaction with endothelin and TGF-β. *J Am Soc Nephrol* 2001; **12**: 2701–2710.
16. Rumble JR, Gilbert RE, Cox A, Wu L, Cooper ME. Angiotensin converting enzyme inhibition reduces the expression of transforming growth factor-beta1 and type IV collagen in diabetic vasculopathy. *J Hypertens* 1998; **16**: 1603–1609.
17. Van Vliet A, Baelde HJ, Vleming LJ, de Heer E, Bruijn JA. Distribution of fibronectin isoforms in human renal disease. *J Pathol* 2001; **193**: 256–262.
18. Colombi M, Barlati S, Kornblihtt A, Baralle FE, Vaheri A. A family of fibronectin mRNAs in human normal and transformed cells. *Biochim Biophys Acta* 1986; **868**: 207–214.
19. Nickeleit V, Kaufman AH, Zagachin L, Dutt JE, Foster CS, Colvin RB. Healing corneas express embryonic fibronectin isoforms in the epithelium, subepithelial stroma, and endothelium. *Am J Pathol* 1996; **149**: 549–558.
20. Castellani P, Dorcaratto A, Pau A, *et al*. The angiogenesis marker ED-B+ fibronectin isoform in intracranial meningiomas. *Acta Neurochir (Wien)* 2000; **142**: 277–282.
21. Khan ZA, Cukiernik M, Gonder J, Chakrabarti S. Oncofetal fibronectin in diabetic retinopathy. *Invest Ophthalmol Vis Sci* 2004; **45**: 287–295.
22. Kuro-o M, Nagai R, Nakahara K, *et al*. cDNA cloning of a myosin heavy chain isoform in embryonic smooth muscle and its

expression during vascular development and in arteriosclerosis. *J Biol Chem* 1991; **266**: 3768–3773.
23. Mise N, Kimura K, Kurabayashi M, *et al*. Angiotensin II enhances glomerular expression of a nonmuscle myosin heavy chain, SMemb, with extracellular matrix accumulation. *Nephron* 2002; **90**: 477–483.
24. Aikawa M, Sivam PN, Kuro-o M, *et al*. Human smooth muscle myosin heavy chain isoforms as molecular markers for vascular development and atherosclerosis. *Circ Res* 1993; **73**: 1000–1012.
25. Makino H, Kashihara N, Sugiyama H, *et al*. Phenotypic modulation of the mesangium reflected by contractile proteins in diabetes. *Diabetes* 1996; **45**: 488–495.
26. Tilton RG, Munsch CL, Sherwood SJ, *et al*. Attenuation of pulmonary vascular hypertension and cardiac hypertrophy with sitaxsentan, an orally active ET_A receptor antagonist. *Pulm Pharmacol Ther* 2000; **13**: 87–97.
27. Wu C, Decker ER, Blok N, *et al*. Acyl substitution at the ortho position of anilides enhances oral bioavailability of thiophene sulfonamides: TBC3214, an ET_A selective endothelin antagonist. *J Med Chem* 2001; **44**: 1211–1216.
28. Hileeto D, Cukiernik M, Mukherjee S, *et al*. Contributions of endothelin-1 and sodium hydrogen exchanger-1 in the diabetic myocardium. *Diabetes Metab Res Rev* 2002; **18**: 386–394.
29. Jensen EB, Gundersen HJ, Osterby R. Determination of membrane thickness distribution from orthogonal intercepts. *J Microsc* 1979; **115**: 19–33.
30. Chen S, Khan ZA, Cukiernik M, Chakrabarti S. Differential activation of NF-κB and AP-1 in mediating endothelin-dependent increased fibronectin synthesis in target organs of diabetic complications. *Am J Physiol Endocrinol Metab* 2003; **284**: E1089–E1097.
31. Vasir B, Reitz P, Xu G, Sharma A, Bonner-Weir S, Weir GC. Effects of diabetes and hypoxia on gene markers of angiogenesis (HGF, cMET, uPA and uPAR, TGF-α, TGF-β, bFGF and Vimentin) in cultured and transplanted rat islets. *Diabetologia* 2000; **43**: 763–772.
32. Kofron M, Demel T, Xanthos J, *et al*. Mesoderm induction in Xenopus is a zygotic event regulated by maternal VegT via TGFbeta growth factors. *Development* 1999; **126**: 5759–5770.
33. Suzuki J, Isobe M, Aikawa M, *et al*. Nonmuscle and smooth muscle myosin heavy chain expression in rejected cardiac allografts. A study in rat and monkey models. *Circulation* 1996; **94**: 1118–1124.
34. Inui T, James AF, Fujitani Y, *et al*. ETA and ETB receptors on single smooth muscle cells cooperate in mediating guinea pig tracheal contraction. *Am J Physiol* 1994; **266**: L113–L124.
35. Jandeleit-Dahm K, Hannan KM, Farrelly CA, *et al*. Diabetes-induced vascular hypertrophy is accompanied by activation of Na(+)-H(+) exchange and prevented by Na(+)-H(+) exchange inhibition. *Circ Res* 2002; **87**: 1133–1140.
36. Alessandri G, Chirivi RG, Castellani P, Nicolo G, Giavazzi R, Zardi L. Isolation and characterization of human tumor-derived capillary endothelial cells: role of oncofetal fibronectin. *Lab Invest* 1998; **78**: 127–128.
37. Hashimoto-Uoshima M, Yan YZ, Schneider G, Aukhil I. The alternatively spliced domains EIIIB and EIIIA of human fibronectin affect cell adhesion and spreading. *J Cell Sci* 1997; **110**: 2271–2280.
38. Takeda Y, Miyamori I, Yoneda T, Takeda R. Production of endothelin-1 from the mesenteric arteries of streptozotocin-induced diabetic rats. *Life Sci* 1991; **8**: 2553–2556.
39. Chakrabarti S, Khan ZA, Cukiernik M, Fukuda G, Chen S, Mukherjee S. Alteration of endothelins: a common pathogenetic mechanism in chronic diabetic complications. *Int J Exp Diabetes Res* 2002; **3**: 217–231.
40. Moreau P, d'Uscio LV, Shaw S, Takase H, Barton M, Luscher TF. Angiotensin II increases tissue endothelin and induces vascular hypertrophy: reversal by ET_A-receptor antagonist. *Circulation* 1997; **96**: 1593–1597.
41. Weigert C, Brodbeck K, Klopfer K, Häring HU, Schleicher ED. Angiotensin II induces human TGF-β1 promoter activation: similarity to hyperglycaemia. *Diabetologia* 2002; **45**: 890–898.
42. Rabelink TJ, Bakris GL. The renin-angiotensin system in diabetic nephropathy: the endothelial connection. *Miner Electrolyte Metab* 1998; **24**: 381–388.
43. Cooper ME, Rumble J, Komers R, Du HC, Jandeleit K, Chou ST. Diabetes-associated mesenteric vascular hypertrophy is attenuated by angiotensin-converting enzyme inhibition. *Diabetes* 1994; **43**: 1221–1228.
44. Cao Z, Hulthen UL, Allen TJ, Cooper ME. Angiotensin converting enzyme inhibition and calcium antagonism attenuate streptozotocin-diabetes-associated mesenteric vascular hypertrophy independently of their hypotensive action. *J Hypertens* 1998; **16**: 793–799.
45. Gibbons GH, Pratt RE, Dzau VJ. Vascular smooth muscle cell hypertrophy vs. hyperplasia: autocrine transforming growth factor-beta 1 expression determines growth response to angiotensin II. *J Clin Invest* 1992; **90**: 456–461.
46. Benigni A, Zoja C, Corna D, *et al*. A specific endothelin subtype A receptor antagonist protects against injury in renal disease progression. *Kidney Int* 1993; **44**: 440–444.
47. Ferrer P, Valentine M, Jenkins-West T, *et al*. Orally active endothelin receptor antagonist BMS-182874 suppresses neointimal development in balloon-injured rat carotid arteries. *J Cardiovasc Pharmacol* 1995; **26**: 908–915.
48. Lerman A , Edwards BS, Hallett JW, Heublein DM, Sandberg SM, Burnett JC Jr. Circulating and tissue endothelin immunoreactivity in advanced atherosclerosis. *N Engl J Med* 1991; **325**: 997–1001.
49. Sakai S, Miyauchi T, Kobayashi M, Yamaguchi I, Goto K, Sugishita Y. Inhibition of myocardial endothelin pathway improves long-term survival in heart failure. *Nature* 1996; **384**: 353–355.
50. Depre C, Young ME, Ying J, *et al*. Streptozotocin-induced changes in cardiac gene expression in the absence of severe contractile dysfunction. *J Mol Cell Cardiol* 2000; **32**: 985–996.
51. Mori S, Takemoto M, Yokote K, Asaumi S, Saito Y. Hyperglycemia-induced alteration of vascular smooth muscle phenotype. *J Diabetes Complications* 2002; **16**: 65–68.

